Journal of Medicinal Chemistry



Article

# Quantum Chemistry Calculation-Aided Structural Optimization of Combretastatin A-4-like Tubulin Polymerization Inhibitors: Improved Stability and Biological Activity

Junhang Jiang, Canhui Zheng, Kongkai Zhu, Jia Liu, Nannan Sun, Chongqing Wang, Hualiang Jiang, Ju Zhu, Cheng Luo, and Youjun Zhou

*J. Med. Chem.*, **Just Accepted Manuscript** • DOI: 10.1021/acs.jmedchem.5b00118 • Publication Date (Web): 17 Feb 2015

# Quantum Chemistry Calculation-Aided Structural Optimization of Combretastatin A-4-like Tubulin Polymerization Inhibitors: Improved Stability and Biological Activity

*Junhang Jiang,*[a,†] *Canhui Zheng,*[a,†,*] *Kongkai Zhu,*[b,†] *Jia Liu,*[a] *Nannan Sun,*[a] *Chongqing Wang,*[a] *Hualiang Jiang,*[b,c] *Ju Zhu,*[a,*] *Cheng Luo,*[b,*] *and Youjun Zhou*[a,*]

[a]School of Pharmacy, Second Military Medical University, Shanghai 200433, China.

[b]State Key Laboratory of Drug Research, Shanghai Institute of Materia Medica, Chinese Academy of Sciences, Shanghai 201203.

[c]School of Life Science and Technology, Shanghai Tech University, Shanghai 200031, China

KEYWORDS: stilbenoids, combretastatin A-4, tubulin polymerization inhibitors, cis-trans photoisomerization, quantum chemistry calculation

ABSTRACT: A potent combretastatin A-4 (CA-4) like tubulin polymerization inhibitor **22b** was found with strong anti-tumor activity previously. However, they easily undergo *cis-trans* isomerization under natural light, and the resulting decrease in activity limits its further

applications. In this study, we used quantum chemistry calculations to explore the molecular basis of its instability. Aided by the calculations, two round of structural optimization of **22b** were conducted. Accelerated quantitative light stability testing confirmed that the stability of these designed compounds was significantly improved as predicted. Among them, compounds **1** and **3b** displayed more potent inhibitory activity on tumor cell growth than **22b**. In addition, the potent *in vivo* antitumor activity of compound **1** was confirmed. Quantum chemistry calculations were used in the optimization of stilbene-like molecules, providing new insight into stilbenoid optimization and important implications for the future development of novel CA-4-like tubulin polymerization inhibitors.

## Introduction

Stilbenoids are abundant in natural products and are divided into *Z*-type and *E*-type based on the configuration of their central double bond.[1-5] Key examples include combretastatins (Chart 1) and resveratrol.[1, 6] Combretastatins are strong tubulin polymerization inhibitors binding to the colchicine site and can strongly block tumor growth with a vascular-disrupting effect.[1, 7-9] Several derivates of combretastatin A-4 (CA-4) have entered clinical trials. It is well-known that, for the CA-4-like tubulin polymerization inhibitors, two hydrophobic rings (rings A and B) in the *Z*-configuration of the linking bridge were necessary to bind to the active site.[7, 8, 10, 11] However, these compounds have a central double bond that can undergo *cis-trans* isomerization, greatly changing their overall configuration and, as a consequence, reducing their biological activity.[11-13]

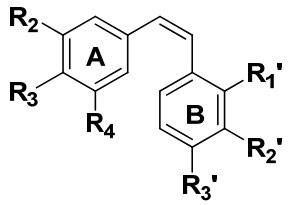


| | $R_1$ | $R_2$ | $R_3$ | $R_1'$ | $R_2'$ | $R_3'$ |
|---|---|---|---|---|---|---|
| **CA-4** | $OCH_3$ | $OCH_3$ | $OCH_3$ | H | OH | $OCH_3$ |
| **CA-1** | $OCH_3$ | $OCH_3$ | $OCH_3$ | OH | OH | $OCH_3$ |
| **CA-2** | $OCH_2O$ | | $OCH_3$ | H | OH | $OCH_3$ |
| **CA-3** | OH | $OCH_3$ | $OCH_3$ | H | OH | $OCH_3$ |

**Chart 1.** The structures of combretastatins.

In our early study,[14] we found a new CA-4-like tubulin polymerization inhibitor **22b** (Scheme 1). It also has two hydrophobic rings in the Z-configuration of the linking bridge similar to CA-4, and showed a similar binding mode to the tubulin protein. The **22b** compound has a strong affinity to tubulin and shows strong anti-tumor activity, which has been confirmed *in vivo*. Its relatively low toxicity also makes it an active compound worthy of further study.[14] However, we found later that it is prone to *cis-trans* isomerization under natural light to yield *Z*-**22b** (Scheme 1). The *E* and *Z* populations achieved equilibrium in dimethylsulfoxide (DMSO) solution after 7 days, and the *Z*-isomer showed greatly reduced biological activity. This easy isomerization limits the utilization and storage of **22b**.

Theoretical calculations have significantly contributed to drug discovery and design.[15] Because of their high accuracy, quantum mechanical methods have been used in all phases of computer-aided drug design and development,[16] especially in facilitating drug lead discovery and lead optimization. For example, free energy-guided molecular design has been successfully applied in lead optimization for non-nucleoside inhibitors of human immunodeficiency virus (HIV)-1

reverse transcriptase.[17] However, no efficient quantum mechanical methods have been reported for the optimization of CA-4-like tubulin polymerization inhibitors.

In this study, we used time-dependent density functional theory (TD-DFT) calculations to explore the mechanism of the easy *cis-trans* photoisomerization of **22b**. Aided by the quantum chemistry calculation, two round of structural optimization of **22b** were conducted. Accelerated quantitative light stability testing and ultraviolet-visible spectrophotometric analysis confirmed that the stability of these designed compounds was significantly improved as predicted. Among them, compounds **1** and **3b** displayed more potent inhibitory activity on tumor cell growth than **22b**. In addition, the potent *in vivo* antitumor activitiy of compound **1** was confirmed, encouraging further study of these designed anti-tumor compounds. Quantum chemistry calculations were used in the optimization of stilbene-like molecules, providing new insight into stilbenoid optimization and important implications for the future development of novel CA-4-like tubulin polymerization inhibitors.

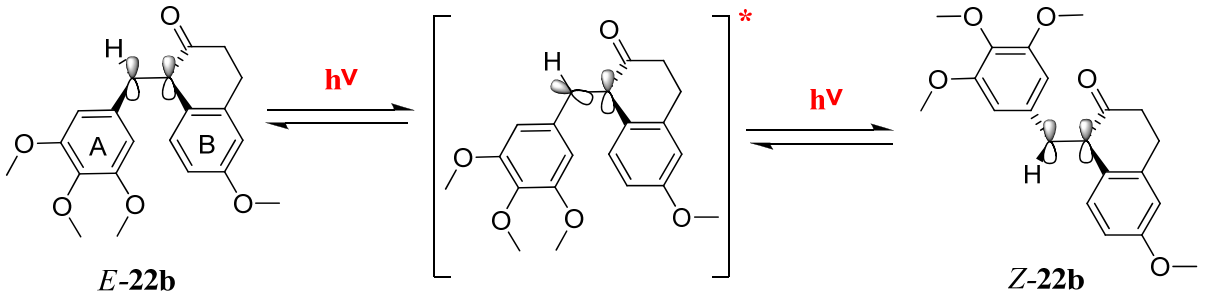


**Scheme 1.** The *cis–trans* photoisomerization of **22b**

## Results and discussions

**Quantum chemical calculations.** According to the literature,[18-23] the *cis-trans* isomerization of stilbenoids is photoinduced. In this isomerization process, the electron might be excited from the

ground state (S0) to an excited state (Scheme 1). Electron transitions mainly occur between the first excited state (S1) and the ground state.[24, 25] As illustrated in Table 1, TD-DFT at the B3LYP/6-31+G(d) and B3LYP/6-311++G(d,p) levels was employed to calculate the vertical excitation energy of molecule **22b** in Gaussian 09.[26] The vertical transition from S0 to S1 in **22b** was found to be an optically allowed $\pi \rightarrow \pi^*$ with an oscillator strength of 0.2983 by TD-DFT/B3LYP/6-31+G(d), which represents the transition from the highest occupied molecular orbital (HOMO) to the lowest unoccupied molecular orbital (LUMO) (Figure 1). Analysis of the frontier orbitals determined that this transition was mainly located on the double bond linking the phenyl moieties. As indicated by this calculation, the wavelength required for the vertical excitation of **22b** is in the visible spectrum, allowing it to be quickly isomerized in natural light. The energy gap between the HOMO and LUMO (Table 3) of **22b** is also an indicator of its instability.

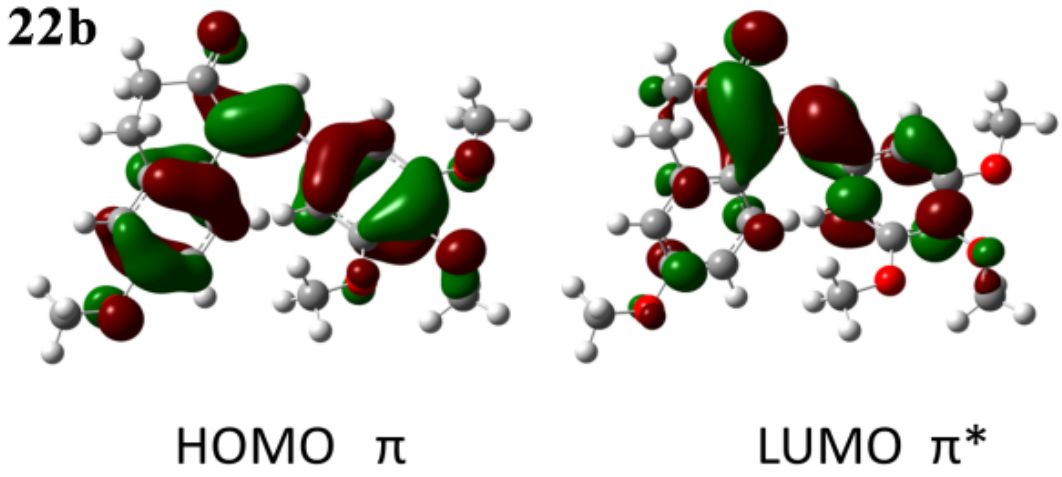


**Figure 1.** The frontier orbitals of **22b** involved in the S0→S1 transitions

**Table 1**. The vertical excitation energies and excitation wavelengths of the four lowest excited states of **22b**

| State | B3LYP (6-31+G(d)) | | | B3LYP (6-311++G(d,p)) | | |
|---|---|---|---|---|---|---|
| | $E_{ex}$ (eV) | os | λ (nm) | $E_{ex}$ (eV) | os | λ (nm) |
| S1 | 3.0783 | 0.2983 | 402.77 | 3.0889 | 0.2921 | 401.39 |
| S2 | 3.4556 | 0.0767 | 358.80 | 3.4754 | 0.0736 | 356.75 |
| S3 | 3.5335 | 0.0736 | 350.88 | 3.5564 | 0.0738 | 348.62 |
| S4 | 3.9428 | 0.0501 | 314.46 | 3.9656 | 0.0481 | 312.65 |

$E_{ex}$ is the vertical excitation energy in eV; os is the oscillator strength; λ is the excitation wavelength in nm.

**Table 2.** Vertical transition excitation energies (S0 to S1) of the eight compounds

| | S0→S1 (6-31+G(d)) | | S0→S1 (6-311++G(d,p)) | |
|---|---|---|---|---|
| | $E_{ex}$ (eV) | λ (nm) | $E_{ex}$ (eV) | λ (nm) |
| **22b** | 3.0783(0.2983) | 402.77 | 3.0889(0.2921) | 401.39 |
| CA-4 | 3.7023(0.4311) | 334.89 | 3.7240(0.3884) | 332.93 |
| **1** | 3.7939(0.2909) | 326.80 | 3.7979(0.2750) | 326.46 |
| **2** | 3.7940(0.2909) | 326.79 | 3.7979(0.2750) | 326.45 |
| **3a** | 3.7310(0.3781) | 332.31 | 3.7440(0.3594) | 331.15 |
| **3b** | 3.6571(0.3926) | 339.02 | 3.6704(0.3710) | 337.79 |
| **4a** | 3.8665(0.3242) | 320.66 | 3.8812(0.3070) | 319.45 |
| **4b** | 3.8210(0.3617) | 324.48 | 3.8352(0.3449) | 323.28 |

$E_{ex}$ is the vertical excitation energy in eV with oscillator strength in parentheses; λ is the wavelength in nm.

**Table 3.** The energy gaps between the HOMO and LUMO orbitals of the eight compounds

| | HOMO | | LUMO | | Energy Gap | |
|---|---|---|---|---|---|---|
| | 6-31+G(d) | 6-311++G(d,p) | 6-31+G(d) | 6-311++G(d,p) | 6-31+G(d) | 6-311++G(d,p) |
| **22b** | -0.205 63 | -0.20715 | -0.07735 | -0.07801 | 0.12828 | 0.12914 |
| CA-4 | -0.19894 | -0.20122 | -0.04790 | -0.04838 | 0.15104 | 0.15284 |
| **1** | -0.19608 | -0.19812 | -0.03875 | -0.04026 | 0.15733 | 0.15786 |
| **2** | -0.19608 | -0.19812 | -0.03875 | -0.04026 | 0.15733 | 0.15786 |
| **3a** | -0.20266 | -0.20469 | -0.04910 | -0.05017 | 0.15356 | 0.15452 |
| **3b** | -0.20574 | -0.20829 | -0.05517 | -0.05668 | 0.15057 | 0.15161 |
| **4a** | -0.20251 | -0.20474 | -0.04265 | -0.04392 | 0.15986 | 0.16082 |
| **4b** | -0.20606 | -0.20884 | -0.04846 | -0.05024 | 0.1576 | 0.1586 |

The energy unit is hartree where 1 hartree = 27.2114 eV.

As seen from the LUMO, the carbonyl group and the central double bond linking the phenyl moieties contribute most to the π* orbital. Consequently, if the carbonyl group is changed to a group with no double bond, the energy of the LUMO could be decreased and the energy gap between the HOMO and LUMO could be increased, thereby increasing the stability of the molecule. And with respect to conjugation, if the carbonyl group was changed to a group with no double bond, the conjugation of the entire molecule could be decreased, which could increase the excited state energy. Increased excited state energy could also make the molecule more stable. Guided by this analysis, two optical isomers (*S* isomer **1** and *R* isomer **2**, Scheme 2) were designed by changing the carbonyl group in **22b** to a hydroxyl group. A similar approach was used to calculate the vertical excitation energies of optical isomers **1** and **2** (Table 2)**.** The results

showed that the two excitation energies were almost identical. Both were significantly higher than **22b** and were even slightly higher than CA-4. As expected, the excitation wavelength needed for isomerization was significantly shortened. The energy gaps between the HOMO and LUMO (Table 3) of these two molecules also indicated their increased stability. In addition, they may have similar biological activity to **22b** due to the minimal change in their spatial configuration. Besides, in order to further testify our conjecture, we also calculated the vertical excitation energy and energy gaps between the HOMO and LUMO of another compound, which designed by changing the carbonyl group to -C=N-NH2, retaining the double bond. The data (not shown) indicated that the stability of this compound is not significantly increased compared to **22b**.

After calculation, these two compounds **1** and **2** were synthesized and their stabilities were confirmed to be improved relative to **22b** (see below). Then, another two optical isomers (*S* isomer **3a** and *R* isomer **4a**, Scheme 2) were designed by changing the connection between the six-membered ring of **1** and **2** from the B ring to the A ring. These compounds could have similar improved stability, because their core skeleton (*E*)-1-benzylidene-1,2,3,4-tetrahydronaphthalen-2-ol were identical. It was confirmed by the theoretical study, which showed that the vertical excitation energy of compounds **3a** and **4a** were equivalent to that of compounds **1** and **2**, and significantly higher than **22b** (Table 2 and 3). In addition, they also have two hydrophobic rings in the *Z*-configuration of the linking bridge, similar to CA-4, and may have similar biological activity.

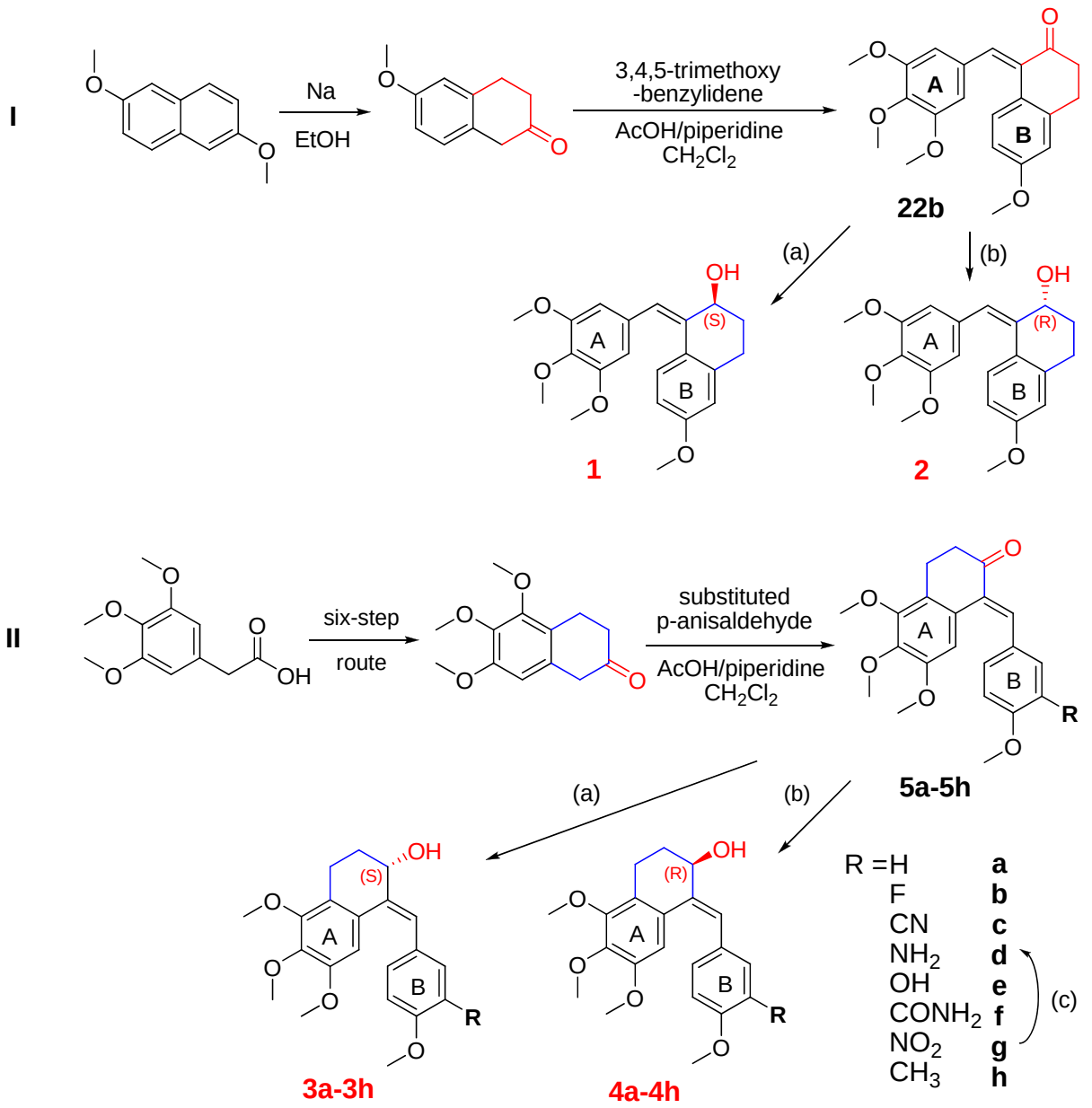


**Scheme 2.** Synthesis of target compounds. Reagents and conditions: (a) $BH_3$•$Me_2S$, (*R*)-(+)-2-methyl-CBS-oxazaborolidine, anhydrous THF, -20 °C; 1 h, 77% - 93%; (b) $BH_3$•$Me_2S$, (*S*)-(-)-2-methyl-CBS-oxazaborolidine, anhydrous THF, -20 °C; 1 h, 78% - 87%; (c) Fe powder, AcOH, 75% EtOH, 70 °C, 0.5 h, 83% and 85% respectively.

**Chemical synthesis.** The *E* isomer **22b** was prepared by the Knoevenagel reaction from the key intermediate 6-methoxy-3,4-dihydronaphthalen-2(1*H*)-one according to our prior work.[14, 27] Based on the high enantio-selectivity of the Corey-Bakshi-Shibata (CBS) catalysts, the CBS reduction was selected to produce compounds **1** and **2** (Scheme 2 I)**.** Compound **22b** was treated with borane-methyl sulfide complex catalyzed by (*R*)-(+)-2-methyl-CBS-oxazaborolidine in anhydrous THF at -20 °C to yield *S* isomer **1** (93% yield, ee: 98.53%). Similarly, *R* isomer **2** was obtained using (*S*)-(-)-2-methyl-CBS-oxazaborolidine (87% yield, ee: 95.76%). Single crystal X-ray analysis data verified their absolute configurations.

The synthetic route to the key intermediate of **22b** could not be used to prepare 5,6,7-trimethoxy-3,4-dihydronaphthalen-2(1*H*)-one, the key intermediate of compound **5**, because the corresponding starting materials were not commercially available. We used a more indirect route (six steps) to afford it, which then was reacted with substituted panisaldehydes to afford compound **5** (Scheme 2 II).[28] We prepared enantiomers **3a**-**3h** and **4a**-**4h** using the same methods as in the synthesis of **1** and **2**. The CBS reduction gave good yields (77% to 93%) and high enantiomeric excesses (87% ee to 99% ee).

**Light stability test and ultraviolet-visible spectrophotometric analysis.** Stability testing experiments were conducted to confirm our predictions. More than a week was needed for compound **22b** to reach *cis-trans* isomerization equilibrium under natural light, and this time changed with the light intensity. Thus, accelerated quantitative stability testing was performed with a high-power xenon lamp and a visible light filter. We used this equipment to irradiate samples **22b**, **1**, **2**, **3a**, **4a** and CA-4 in DMSO. HPLC was used to analyze the sample changes and LC-HRMS to determine the sample structures.[29] After irradiation, the *Z*-configuration

isomers of these compounds were produced with content changes as a function of irradiation time as shown in Figure 2.

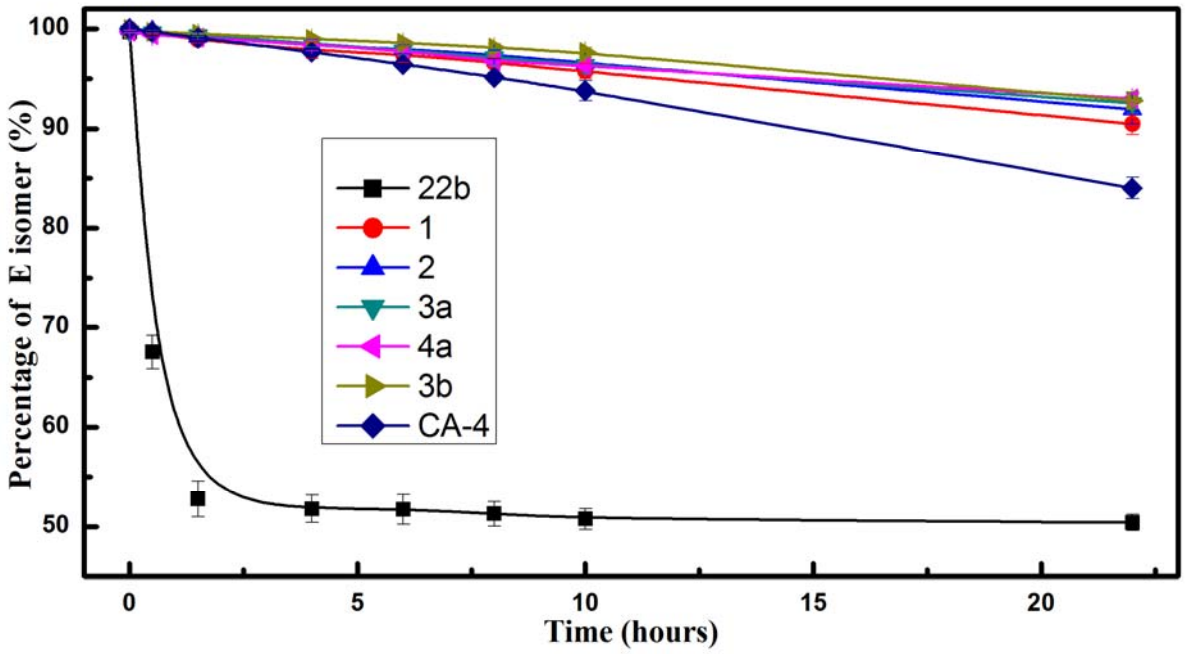


**Figure 2.** Changes in the seven compounds over time after visible light irradiation. Data are expressed as the mean ± SD of the percentage of *E* isomer at each time point.

The results showed that *cis-trans* isomerization equilibrium of **22b** was achieved after 1.5 hours with 52.8% of **22b** remaining. However, the change in **1**, **2**, **3a** and **4a** was markedly slower than **22b** and was even slower than CA-4. There were 98.9%, 99.2%, 99.4% 99.1% and 99.1% of **1**, **2**, **3a**, **4a** and CA-4 remaining after 1.5 hours, and 90.2%, 92.0%, 92.6%, 93.0%, and 84.0% remaining after 22 hours, respectively. Indeed, there was no obvious change in these compounds even after 7 days under natural light. The above results were consistent with our expectations. The *cis-trans* isomerization stability of compounds **1**, **2**, **3a** and **4a** was substantially improved relative to **22b** and CA-4 under natural light.

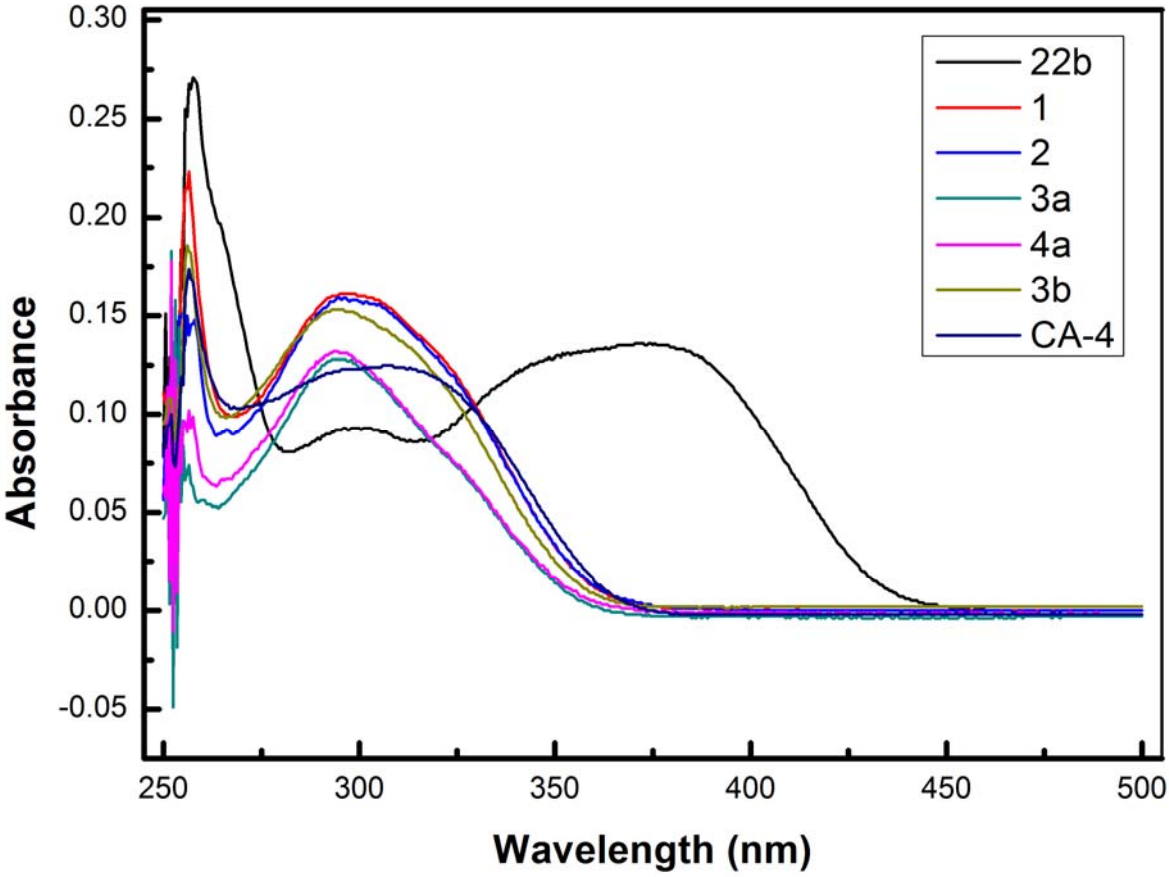


**Figure 3.** The UV-vis absorption spectra of the seven compounds

The UV-vis absorption spectra of the compounds indicate at which wavelengths they can excite their electrons to higher anti-bonding molecular orbitals.[30] Thus, we used UV-vis spectrophotometry to analyze samples **22b**, **1**, **2**, **3a**, **4a** and CA-4 in DMSO. The results (Figure 3) showed that compound **22b** had a broad absorption peak at 375.5 nm that covered a large range of the wavelengths in the visible region. In contrast, the absorption peaks of **1**, **2**, **3a**, and **4a** were shifted to shorter wavelengths than **22b** (299.0, 296.5, 296.5, and 294.5 nm, respectively). These wavelength peaks were even slightly shorter than for CA-4, which is near 308.5 nm. These results were consistent with our theoretical calculations. The UV-vis absorption

spectra of compounds **1**, **2**, **3a**, and **4a** did not overlap with any of the wavelengths in the visible range. Thus, their electron transitions were difficult to excite using visible light. Consequently, their *cis-trans* isomerization under natural light was markedly decreased.

**Biological Activity *in vitro*.** We evaluated the biological activities of compounds **1**, **2**, **3a** and **4a**, which had improved stability relative to **22b**, on the HT-29 human colon cancer and SKOV3 human ovarian cancer cell line (Table 4). Compound **1** showed high inhibition of tumor cell growth, even higher than **22b**, and equivalent inhibition to CA-4 in the HT-29 cell line. However, its enantiomer compound **2** exhibited only middling activity. These results suggested that the chirality of the hydroxyl group had little effect on the compounds' stability but a significant effect on their biological activity. The *S* isomer was favorable with respect to biological activity. However, compounds **3a** and **4a** unexpectedly showed only moderate tumor cell growth inhibitory activity. It suggested that the change in the connection between the six-membered ring from B ring to A ring reduced the biological activity. The evaluation of the inhibition of tubulin polymerization showed similar results (Table 5). The docking binding mode of these compounds (Figure S28) could mainly explain the observed structure-activity relationships.

**Table 4.** The tumor cell growth inhibitory activities of the target compounds

| Compd. | Inhibition of tumor cell growth ($IC_{50}$, μM) | |
|---|---|---|
| | HT-29 | SKOV3 |
| CA-4 | 0.001 | 0.001 |
| **22b** | 0.13 ± 0.015 | 0.002 |
| **1** | 0.001 | 0.001 |
| **2** | 0.90 ± 0.083 | 2.02 ± 0.21 |

| | | |
|---|---|---|
| **3a** | 2.46 ± 0.12 | 7.03 ± 0.59 |
| **4a** | 2.60 ± 0.28 | 3.78 ± 0.43 |
| **3b** | 0.003 ± 0.001 | 0.001 |
| **3c** | 0.005 ± 0.001 | 0.02 ± 0.003 |
| **3d** | 0.16 ± 0.026 | 0.74 ± 0.056 |
| **3e** | 0.26 ± 0.059 | 1.06 ± 0.11 |
| **3f** | 0.55 ± 0.10 | 1.44 ± 0.37 |
| **3g** | 1.59 ± 0.21 | 4.64 ± 0.64 |
| **3h** | 2.56 ± 0.36 | 0.73 ± 0.11 |
| **4b** | 0.22 ± 0.028 | 0.72 ± 0.12 |
| **4c** | 0.20 ± 0.013 | 0.60 ± 0.087 |
| **4d** | 0.91 ± 0.085 | 1.87 ± 0.13 |
| **4e** | 0.79 ± 0.098 | 1.59 ± 0.08 |
| **4f** | 0.55 ± 0.081 | 1.92 ± 0.078 |
| **4g** | >10 | >10 |
| **4h** | 3.97 ± 0.54 | 1.34 ± 0.69 |

$IC_{50}$ values are the mean of at least three independent determinations.

**Table 5.** The tubulin assembly inhibitory activities of the target compounds

| Compd. | CA-4 | **22b** | **1** | **2** | **3a** | **4a** | **3b** |
|---|---|---|---|---|---|---|---|
| $IC_{50}$ ± SD (μM) | 1.77± 0.42 | 3.93± 0.40 | 0.41± 0.08 | >10 | >10 | >10 | 5.7± 0.60 |

**Second round of structural optimization.** We then conducted a second round of structural optimization of compounds **3a** and **4a** to improve their biological activity while maintaining their stability. According to the structure-activity relationship of CA-4-like tubulin polymerization

inhibitors, diverse substituents were introduced into the position 3 of the B ring, the change of which has an obvious effect on antitumor activity.[7, 8, 31, 32] Take isomerize compounds **3b** and **4b** with fluorine substituted at position 3 for example, the results of the calculations (Table 2 and Table 3) showed that the vertical excitation energies and the excitation wavelengths needed to these compounds were similar to compounds **3a** and **4a**. They were also predicted to have similar stability in natural light. The diverse substituted *S* isomer compounds **3b-3h** and *R* isomer compounds **4b-4h** were prepared using similar synthetic routes (Scheme 2 II). The biological activity evaluations of these compounds (Table 4) showed that the compounds **3** and **4** with fluorine, cyan, amino and hydroxyl substituted on position 3 showed higher inhibition activities of tumor cell growth than **3a** and **4a**, respectively. Furthermore, compound **3b** had higher activity than **22b** and equivalent activity to CA-4, and compound **3c** had higher activity than **22b** in the HT-29 cell line. The activities of tubulin polymerization of compound **3b** were also improved relative to that of **3a** (Table 5). The docking binding mode of compound **3b** (Figure S28) suggested that the substituent on the position 3 of the B ring could form additional interaction with α subunit of tubulin. The accelerated quantitative light stability testing and UV-vis spectrophotometric analysis confirmed that the stability of compound **3b** was also improved, and its excitation wavelengths were substantially reduced relative to **22b** and CA-4 (Figures 2 and 3).

**Biological Activity *in vivo*.**

Because compound **1** had a slightly higher calculated vertical excitation energy and tubulin assembly inhibitory activity than **3b**, it was selected to further determine the *in vivo* antitumor activitiy in the human colon cancer HT-29 xenograft model. CA-4 and cyclophosphamide (CTX)

were chosen as the reference and positive control. The doses of 50, 150 mg/kg for compound **1** and 50 mg/kg for CA-4 were chosen. As shown in Figure 4 and Table 6, obviously and dose-dependently antitumor effects were observed in mice treated with compound **1** on day 18, which was administered intraperitoneally (ip) once a day. At the dose of 150 mg/kg, compound **1** achieved a T/C ratio of 37%, lower than 52% of CA-4 at the dose of 50 mg/kg. However, the loss of the body weight in animals treated with compound **1** was not obvious than that of CA-4 at this dose. The antitumor potency of compound **1** seemed higher than the lead compound **22b**, which achieved a similar T/C ratio at the dose of 150 mg/kg with that of CA-4 at the dose of 50 mg/kg in our early study. [14]

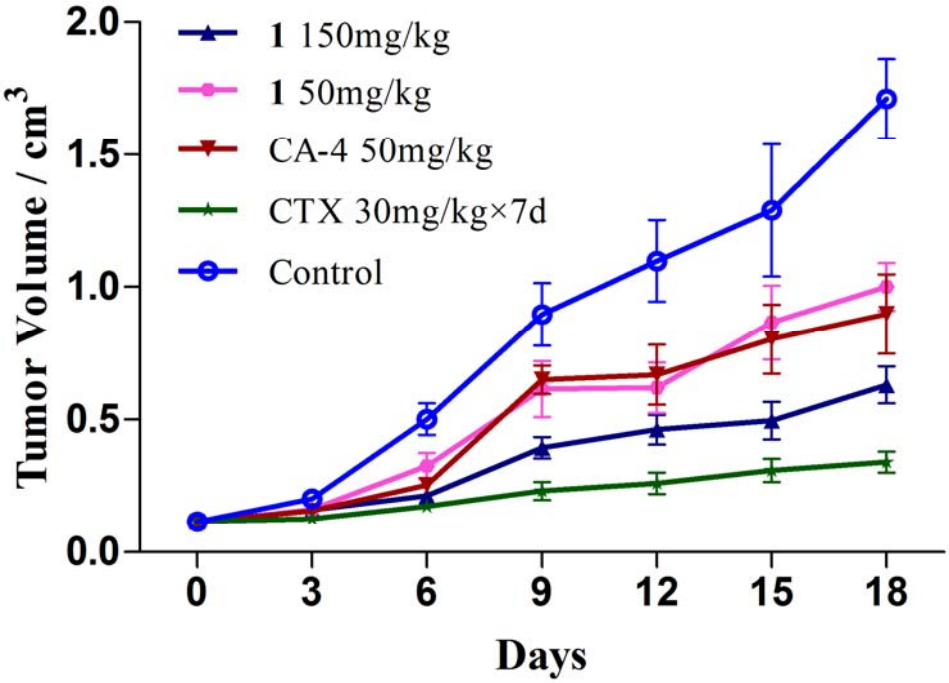


**Figure 4.** The *in vivo* antitumor activitiy of compound **1**. HT-29 tumor-bearing nude mice were administered 150 mg/kg, 50mg/kg of compound **1** or 50mg/kg of CA-4 or vehicle alone

intraperitoneally once a day. The figure shows the tumor volume recorded at the indicated days after treatments. Data are expressed as mean ± SEM of tumor volume at each time point.

**Table 6**. Inhibition of human xenograft growth in vivo by compound 1.

| Compd. | Dosing schedule (mg/kg) | Mice (n) d0/d18 | Tumor volume (mean ± SD, $cm^3$) | | RTV Vt/Vo | T/C (%) | Body weight (mean ± SD, g) | | Body weight change (mean, g) |
|---|---|---|---|---|---|---|---|---|---|
| | | | Vo (d0) | Vt (d18) | | | d0 | d18 | |
| **1** | 150×18d | 6/6 | 0.116±0.012 | 0.630±0.07** | 5.4 | 37 | 23.3±0.95 | 25.1±1.06 | 1.8 |
| **1** | 50×18d | 6/6 | 0.112±0.01 | 1.0±0.09** | 8.9 | 61 | 22.3±0.93 | 24.6±0.63 | 2.3 |
| CA-4 | 50×18d | 6/6 | 0.116±0.01 | 0.897±0.15** | 7.7 | 52 | 22.6±0.96 | 24.3±1.06 | 1.7 |
| CTX | 30×7d | 6/6 | 0.117±0.02 | 0.34±0.04** | 2.9 | 20 | 22.8±0.98 | 23.4±1.08 | 0.6 |
| Control | vehicle×18d | 12/12 | 0.116±0.01 | 1.71±0.15 | 14.7 | / | 22.8±1.01 | 25.3±1.04 | 2.5 |

Data are expressed as mean ± SEM *$P$<0.05, **$P$<0.01 vs. control.

## Conclusion

In conclusion, **22b** is a potent tubulin polymerization inhibitor but with poor stability. It easily undergoes *cis-trans* isomerization under natural light, which limits its applications. In this study, we explored the molecular basis of its instability by TD-DFT calculations and conducted two rounds of structural optimizations aided by quantum chemistry calculations. Its carbonyl was reduced to a hydroxyl to give the *S*-configuration compound **1** and *R*-configuration compound **2**. Then the connection of its six-membered ring was changed from the B ring to the A ring to produce compounds **3a-3h** and **4a-4h**.

As predicted, the accelerated quantitative light-stability testing and UV-vis spectrophotometric analysis results showed that the excitation wavelengths of our purposefully designed compounds was reduced, and their stability under natural light was improved relative to both **22b** and CA-4. The inhibitory activity evaluation of tumor cell growth and tubulin polymerization revealed improved results for compounds **1** and **3b** relative to **22b**. In addition, the potent *in vivo* antitumor activitiy of compound **1** was confirmed, encouraging further study of these designed anti-tumor compounds.

Stilbenoids are natural compounds with a variety of important biological activities, but the photoisomerization problem has been a common challenge in optimization work. Most quantum chemistry calculation research has focused on the mechanisms of photoisomerization but has not been concerned about optimizing these compounds to improve their stability and maintain their biological activity. The methods we used in this study offer an important framework for future modifications of stilbene-like molecules aided by theoretical calculations to improve their stability.

## Materials and methods

**Chemistry.** Melting points were measured on an electrically heated RK-Z melting point apparatus and are uncorrected. The $^{1}$H nuclear magnetic resonance (NMR) and $^{13}$C NMR spectra were recorded on a Bruker AVANCE III HD 500 MHz (Bruker Biospin, Switzerland) or an AVANCE II600 spectrometer (Bruker Biospin, Switzerland), using trimethylsilyl (TMS) as an internal standard and $CDCl_3$ as the solvent. Chemical shifts are given in ppm ($\delta$), and the spectral data are consistent with the assigned structures. The mass spectra were recorded on a Micromass Qtof-Micro LC−MS or a Bruker MicroToF II ESI LC-MS. Silica gel column chromatography

was performed with silica gel 200-300 mesh. All of the solvents and reagents were analytically pure and, when necessary, were purified and dried using standard protocols. All of the starting materials were commercially available unless otherwise indicated. Yields of purified products were not optimized. The purity of each key compound (>95%) was determined on an Agilent 1100 series liquid chromatography (LC) system (column, ZORBAX Eclipse XDB-C18; mobile phase, methanol (70%)/$H_2O$; UV wavelength, absorbance at 254 nm). The chiral purity of each key compound (>90%) was determined on an Agilent 1100 series LC system (column, CHIRALPAK AD-H; mobile phase, isopropanol (25%)/n-hexane; UV wavelength, absorbance at 254 nm). All of the UV-vis spectroscopic work was carried out on a UV-vis spectrophotometer (SHIMADAZU UV-2600, Japan). The compounds **22b** and **5** were synthesized by the routes we reported previously.[14, 27, 28]

**General procedure for the synthesis of 1, 3a−3c and 3e−3h.** A solution of **22b** or **5** (0.71 mmol) in tetrahydrofuran (THF) (1 mL) was added dropwise slowly at -20 °C under a nitrogen atmosphere to a mixture of 0.14 mL (0.14 mmol) of a 1.0 M toluene solution of (*R*)-(+)-2-methyl-CBS-oxazaborolidine and 0.7 mL (0.70 mmol) of a borane-methyl sulfide complex of a 2.0 M toluene solution in anhydrous THF (3 mL). The reaction mixture was stirred at -20 °C for 1 h and was quenched by the addition of 4 mL of methanol followed by 20 mL of saturated sodium bicarbonate. The mixture was extracted with ethyl acetate (2×100 mL). The combined organic phase was washed with brine, dried over $Na_2SO_4$, filtered, and concentrated in vacuo. The residue crude was purified by flash column chromatography (gradient elution: petroleum ether/ethyl acetate, 0−80%) to obtain the pure product.

**General procedure for the synthesis of 1, 3a−3c and 3e−3h.** A solution of **22b** or **5** (0.70 mmol, 1.0 equiv) in tetrahydrofuran (THF) (1 mL) was added dropwise slowly at -20 °C under a

nitrogen atmosphere to a mixture of 0.14 mL (0.14 mmol, 0.2 equiv) of a 1.0 M toluene solution of (*R*)-(+)-2-Methyl-CBS-oxazaborolidine and 0.7 mL (0.70 mmol, 1.0 equiv) of a borane-methyl sulfide complex of a 2.0 M toluene solution in anhydrous THF (3 mL). The reaction mixture was stirred at -20 °C for 1 h and was quenched by the addition of 4 mL of methanol followed by 20 mL of saturated sodium bicarbonate. The mixture was extracted with ethyl acetate (2×100 mL). The combined organic phase was washed with brine, dried over $Na_2SO_4$, filtered, and concentrated in vacuo. The residue crude was purified by flash column chromatography (gradient elution: petroleum ether/ethyl acetate, 0−80%) to obtain the pure product.

**(*S*,*E*)-6-Methoxy-1-(3,4,5-trimethoxybenzylidene)-1,2,3,4-tetrahydronaphthalen-2-ol (1).** White needles from hexane/ethyl acetate, yield 93%, mp 125−126 °C; High-performance LC (HPLC): 99.05%, ee: 98.53%, tR: 11.4 min (major), 13.3 min (minor); $^1$H NMR (500 MHz, $CDCl_3$) δ 7.26 (d, *J* = 8.7 Hz, 1H), 6.66 (d, *J* = 2.5 Hz, 1H), 6.53 – 6.52 (m, 3H), 6.50 (dd, *J* = 8.8, 2.7 Hz, 1H), 4.52 (dd, *J* = 6.3, 3.3 Hz, 1H), 3.85 (s, 3H), 3.76 (s, 3H), 3.71 (s, 6H), 3.14 – 2.82 (m, 2H), 2.23 – 2.05 (m, 2H), 1.74 (b, 1H); $^{13}$C NMR (125 MHz, $CDCl_3$) δ 159.23, 153.07, 139.38, 139.06, 137.13, 133.29, 131.45, 124.64, 122.78, 112.83, 111.59, 106.32, 72.73, 60.96, 56.06, 55.19, 31.50, 26.26; HRMS (ES+) m/z found 357.1698 ($M+H^+$), while $C_{21}H_{25}O_5$ ($M+H^+$) requires 357.1697.

**(*S*,*E*)-5,6,7-Trimethoxy-1-(4-methoxybenzylidene)-1,2,3,4-tetrahydronaphthalen-2-ol (3a).** White solid, yield 83%, mp 66−67°C; HPLC: 99.15%, ee: 90.32%, tR: 9.4 min (major), 12.7 min (minor); $^1$H NMR (600 MHz, $CDCl_3$) δ 7.26 (dd, J = 8.9, 0.7 Hz, 2H), 6.83 (d, J = 8.8 Hz, 2H), 6.65 (s, 1H), 6.63 (s, 1H), 4.53 (dd, J = 5.9, 3.0 Hz, 1H), 3.90 (s, 3H), 3.88 (s, 3H), 3.81 (s, 3H), 3.37 (s, 3H), 2.98 -2.84 (m, 2H), 2.19 – 2.09 (m, 2H), 1.69 (b, 1H); $^{13}$C NMR (125 MHz, $CDCl_3$)

δ 158.55, 150.86, 150.58, 141.71, 138.41, 130.50, 130.30, 127.52, 123.99, 123.40, 113.73, 108.90, 72.45, 60.75, 60.31, 55.29, 31.14, 20.03; HRMS (ES+) m/z found 357.1690 ($M+H^+$), while $C_{21}H_{25}O_5$ ($M+H^+$) requires 357.1697.

**(*S*,*E*)-1-(3-Fluoro-4-methoxybenzylidene)-5,6,7-trimethoxy-1,2,3,4-tetrahydronaphthalen-2-ol (3b).** White solid, yield 86%, mp 106−107 °C; HPLC: 99.49%, ee: 99.40%, tR: 6.4 min (major), 8.1 min (minor); $^1$H NMR (600 MHz, $CDCl_3$) δ 7.06 (dd, J = 12.5, 2.0 Hz, 1H), 7.02 – 6.98 (m, 1H), 6.85 (t, J = 8.6 Hz, 1H), 6.57 (s, 2H), 4.49 (dd, J = 6.7, 3.0 Hz, 1H), 3.88 (s, 3H), 3.87 (s, 3H), 3.86 (s, 3H), 3.38 (s, 3H), 2.99 – 2.79 (m, 2H), 2.19 – 2.03 (m, 2H), 1.68 (b, 1H); $^{13}$C NMR (150 MHz, $CDCl_3$) δ 152.95, 151.32, 150.96, 150.75, 146.52, 146.45, 142.04, 139.61, 131.09, 131.04, 127.04, 125.44, 124.16, 121.94, 116.87, 116.75, 113.23, 108.83, 72.32, 60.79, 60.34, 56.35, 55.43, 31.23, 20.13; HRMS (ES+) m/z found 375.1600 ($M+H^+$), while $C_{21}H_{24}FO_5$ ($M+H^+$) requires 375.1603.

**(*S*,*E*)-5-((2-Hydroxy-5,6,7-trimethoxy-3,4-dihydronaphthalen-1(2*H*)-ylidene)methyl)-2-methoxybenzonitrile (3c).** White powder, yield 80%, mp 150−151 °C; HPLC: 99.93%, ee: 99.14%, $[\alpha]_D^{20}$= -23.158 (*c*=0.38, MeOH), tR: 9.4 min (major), 12.3 min (minor); $^1$H NMR (600 MHz, $CDCl_3$) δ 7.52 (d, J = 2.1 Hz, 1H), 7.46 (dd, J = 8.7, 2.2 Hz, 1H), 6.87 (d, J = 8.8 Hz, 1H), 6.55 (s, 1H), 6.43 (s, 1H), 4.49 (dd, J = 7.4, 2.8 Hz, 1H), 3.92 (s, 3H), 3.89 (s, 3H), 3.87 (s, 3H), 3.36 (s, 3H), 2.99 – 2.80 (m, 2H), 2.23 – 2.13 (m, 1H), 2.08 (td, J = 13.4, 6.8 Hz, 1H), 1.79 (b, 1H). $^{13}$C NMR (150 MHz, $CDCl_3$) δ 159.89, 151.13, 150.88, 142.27, 140.89, 135.51, 134.34, 130.98, 126.74, 124.39, 120.13, 116.22, 111.13, 108.55, 101.68, 72.00, 60.82, 60.35, 56.17, 55.50, 31.38, 20.34; HRMS (ES+) m/z found 382.1648 ($M+H^+$), while $C_{22}H_{24}NO_5$ ($M+H^+$) requires 382.1649.

**(*S*,*E*)-1-(3-Hydroxy-4-methoxybenzylidene)-5,6,7-trimethoxy-1,2,3,4-tetrahydronaphthalen-2-ol (3e).** White solid, yield 84%, mp 108−109 °C, HPLC: 99.72%; $^{1}$H NMR (600 MHz, $CDCl_3$) δ 6.91 (d, J = 2.0 Hz, 1H), 6.80 – 6.73 (m, 2H), 6.64 (s, 1H), 6.58 (s, 1H), 5.56 (s, 1H), 4.49 (dd, J = 6.2, 3.4 Hz, 1H), 3.87 (s, 3H), 3.87 (s, 3H), 3.85 (s, 3H), 3.37 (s, 3H), 2.95 – 2.80 (m, 2H), 2.17 – 2.06 (m, 2H), 1.73 (b, 1H); $^{13}$C NMR (150 MHz, $CDCl_3$) δ 150.80, 150.58, 145.55, 145.37, 141.80, 138.61, 131.26, 127.31, 124.00, 123.47, 121.33, 115.31, 110.51, 109.08, 72.53, 60.78, 60.33, 56.02, 55.39, 31.03, 19.95; HRMS (ES+) m/z found 373.1645($M+H^+$), while $C_{21}H_{25}O_6$ ($M+H^+$) requires 373.1646.

**(*S*,*E*)-5-((2-Hydroxy-5,6,7-trimethoxy-3,4-dihydronaphthalen-1(2*H*)-ylidene)methyl)-2-methoxybenzamide (3f).** White powder, yield 83%, mp 62−63 °C; HPLC: 99.94%, ee: 99.17%, tR: 14.1 min (major), 23.9 min (minor); $^{1}$H NMR (600 MHz, $CDCl_3$) δ 8.17 (d, J = 2.2 Hz, 1H), 7.68 (s, 1H), 7.40 (dd, J = 8.6, 2.2 Hz, 1H), 6.86 (d, J = 8.6 Hz, 1H), 6.63 (s, 1H), 6.52 (s, 1H), 5.87 (s, 1H), 4.51 (dd, J = 6.5, 2.8 Hz, 1H), 3.95 (s, 3H), 3.88 (s, 3H), 3.85 (s, 3H), 3.00 – 2.79 (m, 2H), 2.19 – 2.07 (m, 2H), 1.85 (b, 1H); $^{13}$C NMR (150 MHz, $CDCl_3$) δ 166.82, 156.60, 150.95, 150.63, 141.92, 139.73, 134.29, 133.51, 131.16, 127.25, 124.26, 122.02, 120.64, 111.21, 108.83, 72.22, 60.78, 60.32, 56.13, 55.39, 31.10, 20.15; HRMS (ES+) m/z found 400.1757 ($M+H^+$), while $C_{22}H_{26}NO_6$ ($M+H^+$) requires 400.1755.

**(*S*,*E*)-5,6,7-Trimethoxy-1-(4-methoxy-3-nitrobenzylidene)-1,2,3,4-tetrahydronaphthalen-2-ol (3g).** Light yellow solid, yield 81%, mp 106−107 °C; HPLC: 98.81%, ee: 94.25%, tR: 10.0 min (major), 12.2 min (minor); $^{1}$H NMR (600 MHz, $CDCl_3$) δ 7.80 (d, J = 1.5 Hz, 1H), 7.46 (dd, J = 8.6, 1.7 Hz, 1H), 6.97 (d, J = 8.7 Hz, 1H), 6.57 (s, 1H), 6.49 (s, 1H), 4.50 (dd, J = 7.7, 2.7 Hz, 1H), 3.94 (s, 3H), 3.89 (s, 3H), 3.86 (s, 3H), 3.39 (s, 3H), 2.99 – 2.82 (m, 2H), 2.22 – 2.15 (m, 1H), 2.08 (td, J = 13.4, 6.8 Hz, 1H); $^{13}$C NMR (150 MHz, $CDCl_3$) δ 151.41, 151.16, 150.96,

142.36, 141.29, 139.61, 135.06, 130.54, 126.66, 126.13, 124.41, 119.83, 113.18, 108.43, 72.02, 60.83, 60.36, 56.62, 55.55, 31.41, 20.38; HRMS (ES+) m/z found 402.1541 ($M+H^+$), while $C_{21}H_{24}NO_7$ ($M+H^+$) requires 402.1548.

**(*S*,*E*)-5,6,7-Trimethoxy-1-(4-methoxy-3-methylbenzylidene)-1,2,3,4-tetrahydronaphthalen-2-ol (3h).** White solid, yield 77%, mp 54−55 °C; HPLC: 98.65%, ee: 97.42%, tR: 5.7 min (major), 6.8 min (minor); $^1$H NMR (600 MHz, $CDCl_3$) δ 7.12 – 7.09 (m, 2H), 6.73 – 6.69 (m, 1H), 6.67 (s, 1H), 6.60 (s, 1H), 4.50 (t, J = 4.5 Hz, 1H), 3.88 (s, 3H), 3.85 (s, 3H), 3.81 (s, 3H), 3.34 (s, 3H), 2.96 – 2.77 (m, 2H), 2.14 (s, 3H), 2.14 – 2.09 (m, 2H), 1.60 (b, 1H); $^{13}$C NMR (150 MHz, $CDCl_3$) δ 156.79, 150.81, 150.52, 141.67, 137.81, 131.50, 129.69, 127.82, 127.50, 126.29, 123.97, 109.73, 108.89, 72.68, 60.78, 60.33, 55.38, 55.30, 30.98, 19.89, 16.08; HRMS (ES+) m/z found 371.1854 ($M+H^+$), while $C_{22}H_{27}O_5$ ($M+H^+$) requires 371.1853.

**General procedure for the synthesis of 2, 4a−4c and 4e−4h.** The compounds were synthesized using CBS reduction conditions as previously described in the synthesis of **1, 3a−3c** and **3e−3h**, in which a mixture of **22b** or **5** (0.70 mmol, 1.0 equiv) in THF (1 mL), 0.14 mL (0.14 mmol, 0.2 equiv) of a 1.0 M toluene solution of (*S*)-(-)-2-Methyl-CBS-oxazaborolidine and 0.7 mL (0.70 mmol, 1.0 equiv) of a borane-methyl sulfide complex of a 2.0 M toluene solution in anhydrous THF (3 mL) was used.

**(*R*,*E*)-6-Methoxy-1-(3,4,5-trimethoxybenzylidene)-1,2,3,4-tetrahydronaphthalen-2-ol (2).** White needles from hexane/ethyl acetate, yield 87%, mp 123−124 °C; HPLC: 99.30%, ee: 95.76%, tR: 13.3 min (major), 11.4 min (minor); $^1$H NMR (500 MHz, $CDCl_3$) δ 7.27 (d, *J* = 8.7 Hz, 1H), 6.66 (d, *J* = 2.5 Hz, 1H), 6.54 – 6.53 (m, 3H), 6.50 (dd, *J* = 8.8, 2.7 Hz, 1H), 4.53 (dd, *J* = 6.3, 3.3 Hz, 1H), 3.85 (s, 3H), 3.77 (s, 3H), 3.71 (s, 6H), 3.15 – 2.85 (m, 2H), 2.23 – 2.06 (m, 2H), 1.72 (b, 1H); $^{13}$C NMR (125 MHz, $CDCl_3$) δ 159.23, 153.07, 139.38, 139.06, 137.13,

133.29, 131.46, 124.64, 122.79, 112.82, 111.59, 106.32, 72.73, 60.96, 56.06, 55.18, 31.49, 26.26; HRMS (ES+) m/z found 379.1518 ($M+Na^+$), while $C_{21}H_{24}O_5Na$ ($M+Na^+$) requires 379.1516. X-ray quality crystals were obtained via slow evaporation of an ethyl acetate solution in air. Crystallographic data for **2** (Figure S1 and Table S1) have been deposited in the Cambridge Crystallographic Data Centre as supplementary publication number CCDC 1032584.

**(*R*,*E*)-5,6,7-Trimethoxy-1-(4-methoxybenzylidene)-1,2,3,4-tetrahydronaphthalen-2-ol (4a).** White solid, yield 80%, mp 61−62°C; HPLC: 99.00%, ee: 98.82%, tR: 12.7 min (major), 9.4 min (minor); $^1$H NMR (600 MHz, $CDCl_3$) δ 7.27 (s, 1H), 7.25 (s, 1H), 6.83 (s, 1H), 6.82 (s, 1H), 6.65 (s, 1H), 6.63 (s, 1H), 4.53 (dd, J = 6.0, 3.0 Hz, 1H), 3.90 (s, 3H), 3.88 (s, 3H), 3.81 (s, 3H), 3.37 (s, 3H), 2.99 – 2.83 (m, 2H), 2.20 – 2.10 (m, 2H), 1.70 (b, 1H); $^{13}$C NMR (125 MHz, $CDCl_3$) δ 158.58, 150.87, 150.61, 141.73, 138.37, 130.51, 130.28, 127.47, 123.98, 123.49, 113.74, 108.91, 72.53, 60.76, 60.33, 55.30, 31.12, 19.98; HRMS (ES+) m/z found 357.1691 ($M+H^+$), while $C_{21}H_{25}O_5$ ($M+H^+$) requires 357.1697.

**(*R*,*E*)-1-(3-Fluoro-4-methoxybenzylidene)-5,6,7-trimethoxy-1,2,3,4-tetrahydronaphthalen-2-ol (4b).** White solid, yield 83%, mp 107−108 °C; HPLC: 98.56%, ee: 99.38%, tR: 8.1 min (major), 6.4 min (minor); $^1$H NMR (600 MHz, $CDCl_3$) δ7.06 (dd, J = 12.5, 2.1 Hz, 1H), 7.02 – 7.04 (m, 1H), 6.85 (t, J = 8.6 Hz, 1H), 6.57 (s, 2H), 4.49 (dd, J = 7.0, 2.8 Hz, 1H), 3.88 (s, 3H), 3.87 (s, 3H), 3.86 (s, 3H), 3.38 (s, 3H), 2.98 – 2.78 (m, 2H), 2.20 – 2.03 (m, 2H), 1.69 (b, 1H); $^{13}$C NMR (150 MHz, $CDCl_3$) δ 152.95, 151.32, 150.96, 150.74, 146.51, 146.44, 142.03, 139.61, 131.09, 131.05, 127.05, 125.44, 124.17, 121.94, 116.87, 116.75, 113.23, 108.83, 72.31, 60.79, 60.34, 56.35, 55.43, 31.23, 20.14; HRMS (ES+) m/z found 375.1592 ($M+H^+$), while $C_{21}H_{24}FO_5$ ($M+H^+$) requires 375.1603.

**(*R*,*E*)-5-((2-Hydroxy-5,6,7-trimethoxy-3,4-dihydronaphthalen-1(2H)-ylidene)methyl)-2-methoxybenzonitrile (4c).** White powder, yield 79%, mp 151−152 °C; HPLC: 98.85%, ee: 98.99%, $[\alpha]_D^{20}$ = 20.583 (*c*=0.37, MeOH), tR: 12.3 min (major), 9.3 min (minor); $^1$H NMR (600 MHz, $CDCl_3$) δ7.52 (d, J = 2.1 Hz, 1H), 7.46 (ddd, J = 8.7, 2.2, 0.6 Hz, 1H), 6.87 (d, J = 8.8 Hz, 1H), 6.55 (s, 1H), 6.43 (s, 1H), 4.49 (dd, J = 7.3, 2.5 Hz, 1H), 3.92 (s, 3H), 3.89 (s, 3H), 3.87 (s, 3H), 3.36 (s, 3H), 2.99 – 2.80 (m, 2H), 2.23 – 2.02 (m, 2H), 1.76 (b, 1H); $^{13}$C NMR (150 MHz, $CDCl_3$) δ159.88, 151.13, 150.88, 142.27, 140.90, 135.51, 134.34, 130.98, 126.74, 124.39, 120.12, 116.22, 111.13, 108.55, 101.68, 72.00, 60.82, 60.35, 56.17, 55.50, 31.38, 20.35; HRMS (ES+) m/z found 382.1631 ($M+H^+$), while $C_{22}H_{24}NO_5$ ($M+H^+$) requires 382.1649.

**(*R*,*E*)-1-(3-Hydroxy-4-methoxybenzylidene)-5,6,7-trimethoxy-1,2,3,4-tetrahydronaphthalen-2-ol (4e).** White solid, yield 78%, mp 51−52 °C, HPLC: 98.18%; $^1$H NMR (600 MHz, $CDCl_3$) δ 6.94 (d, J = 2.0 Hz, 1H), 6.82 (dd, J = 8.3, 2.0 Hz, 1H), 6.77 (d, J = 8.3 Hz, 1H), 6.67 (s, 1H), 6.61 (s, 1H), 5.55 (s, 1H), 4.52 (s, 1H), 3.90 (s, 3H), 3.89 (s, 3H), 3.88 (s, 3H), 3.40 (s, 3H), 2.99 – 2.81 (m, 2H), 2.20 – 2.06 (m, 2H), 1.71 (b, 1H); $^{13}$C NMR (150 MHz, $CDCl_3$) δ 150.80, 150.58, 145.56, 145.38, 141.80, 138.62, 131.27, 127.32, 124.00, 123.47, 121.33, 115.31, 110.51, 109.09, 72.53, 60.77, 60.33, 56.02, 55.39, 31.03, 19.95; HRMS (ES+) m/z found 373.1639($M+H^+$), while $C_{21}H_{25}O_6$ ($M+H^+$) requires 373.1646.

**(*R*,*E*)-5-((2-Hydroxy-5,6,7-trimethoxy-3,4-dihydronaphthalen-1(2*H*)-ylidene)methyl)-2-methoxybenzamide (4f).** White powder, yield 82%, mp 61−62 °C; HPLC: 99.64%, ee: 98.38%, tR: 23.8 min (major), 14.2 min (minor); $^1$H NMR (600 MHz, $CDCl_3$) δ 8.17 (d, J = 2.3 Hz, 1H), 7.68 (s, 1H), 7.40 (dd, J = 8.6, 2.3 Hz, 1H), 6.87 (d, J = 8.6 Hz, 1H), 6.63 (s, 1H), 6.52 (s, 1H), 5.84 (s, 1H), 4.51 (dd, J = 6.7, 2.6 Hz, 1H), 3.95 (s, 3H), 3.88 (s, 3H), 3.85 (s, 3H), 3.32 (s, 3H), 2.98 – 2.79 (m, 2H), 2.18 – 2.06 (m, 2H), 1.73 (b, 1H); $^{13}$C NMR (150 MHz, $CDCl_3$) δ 166.85,

156.61, 150.95, 150.63, 141.92, 139.74, 134.29, 133.50, 131.16, 127.26, 124.26, 122.01, 120.64, 111.21, 108.83, 72.21, 60.78, 60.32, 56.13, 55.39, 31.11, 20.16; HRMS (ES+) m/z found 400.1755 ($M+H^+$), while $C_{22}H_{26}NO_6$ ($M+H^+$) requires 400.1755.

**(*R*,*E*)-5,6,7-Trimethoxy-1-(4-methoxy-3-nitrobenzylidene)-1,2,3,4-tetrahydronaphthalen-2-ol (4g).** Light yellow solid, yield 82%, mp 104−105 °C; HPLC: 99.34%, ee: 96.74%, tR: 12.2 min (major), 10.0min (minor); $^1$H NMR (600 MHz, $CDCl_3$) δ 7.80 (d, J = 2.2 Hz, 1H), 7.46 (dd, J = 8.8, 2.1 Hz, 1H), 6.97 (d, J = 8.7 Hz, 1H), 6.57 (s, 1H), 6.49 (s, 1H), 4.50 (dd, J = 6.7, 3.4 Hz, 1H), 3.94 (s, 3H), 3.89 (s, 3H), 3.86 (s, 3H), 3.39 (s, 3H), 2.99 – 2.81 (m, 2H), 2.22 – 2.15 (m, 1H), 2.08 (td, J = 13.4, 6.3 Hz, 1H); $^{13}$C NMR (150 MHz, $CDCl_3$) δ 151.40, 151.15, 150.95, 142.35, 141.30, 139.59, 135.08, 130.55, 126.68, 126.13, 124.41, 119.81, 113.18, 108.43, 71.99, 60.83, 60.36, 56.61, 55.55, 31.40, 20.40; HRMS (ES+) m/z found 402.1541 ($M+H^+$), while $C_{21}H_{24}NO_7$ ($M+H^+$) requires 402.1548.

**(*R*,*E*)-5,6,7-Trimethoxy-1-(4-methoxy-3-methylbenzylidene)-1,2,3,4-tetrahydronaphthalen-2-ol (4h).** White solid, yield 78%, mp 72−73 °C; HPLC: 99.21%, ee: 87.58%, tR: 6.8 min (major), 5.7 min (minor); $^1$H NMR (600 MHz, $CDCl_3$) δ 7.12 – 7.09 (m, 2H), 6.72 (d, J = 9.0 Hz, 1H), 6.67 (s, 1H), 6.60 (s, 1H), 4.50 (t, J = 4.7 Hz, 1H), 3.88 (s, 3H), 3.85 (s, 3H), 3.81 (s, 3H), 3.34 (s, 3H), 2.97 – 2.80 (m, 2H), 2.14 (s, 3H), 2.14 – 2.09 (m, 2H), 1.68 (b, 1H); $^{13}$C NMR (150 MHz, $CDCl_3$) δ 156.79, 150.81, 150.52, 141.67, 137.81, 131.50, 129.69, 127.81, 127.50, 126.29, 123.97, 109.73, 108.89, 72.68, 60.78, 60.33, 55.38, 55.30, 30.98, 19.89, 16.08; HRMS (ES+) m/z found 371.1848 ($M+H^+$), while $C_{22}H_{27}O_5$ ($M+H^+$) requires 371.1853.

**General procedure for the synthesis of 3d and 4d.** A mixture of Fe powder (1.6 mmol, 10.0 equiv) in ethanol (75%, 10 mL) and acetic acid (2 mL) was heated to reflux for one hour then the

compound **3g** or **4g** (0.16 mmol, 1.0 equiv) was added. After 30 min the mixture was filtered through celite and the filtrate was extracted with ethyl acetate (2×50 mL). The combined organic phase was washed with brine, dried over $Na_2SO_4$, filtered, and concentrated in vacuo. The residue crude was purified by flash column chromatography (petroleum ether/ethyl acetate=2:1) to obtain the pure product.

**(*S*,*E*)-1-(3-Amino-4-methoxybenzylidene)-5,6,7-trimethoxy-1,2,3,4-tetrahydronaphthalen-2-ol (3d).** Light pale solid, yield 83%, mp 61−62 °C; HPLC : 98.48%, ee: 97.02%, tR: 11.8 min (major), 17.8 min (minor); $^1$H NMR (600 MHz, $CDCl_3$) δ 6.72 (s, 1H), 6.71 (s, 1H), 6.70 – 6.65 (m, 2H), 6.57 (s, 1H), 4.49 (t, J = 4.8 Hz, 1H), 3.87 (s, 3H), 3.85 (s, 3H), 3.83 (s, 3H), 3.38 (s, 3H), 2.97 – 2.77 (m, 2H), 2.16 – 2.05 (m, 2H); $^{13}$C NMR (150 MHz, $CDCl_3$) δ 150.72, 150.49, 146.48, 141.61, 137.85, 135.69, 130.61, 127.50, 124.22, 123.88, 119.78, 115.66, 110.25, 109.02, 72.62, 60.77, 60.32, 55.58, 55.38, 30.93, 19.88; HRMS (ES+) m/z found 372.1804 ($M+H^+$), while $C_{21}H_{26}NO_5$ ($M+H^+$) requires 372.1806.

**(*R*,*E*)-1-(3-Amino-4-methoxybenzylidene)-5,6,7-trimethoxy-1,2,3,4-tetrahydronaphthalen-2-ol (4d).** Light pale solid, yield 85%, mp 56−58 °C; HPLC : 98.03%, ee: 92.66%, tR: 17.6 min (major), 11.7 min (minor); $^1$H NMR (600 MHz, $CDCl_3$) δ 6.72 (s, 1H), 6.70 – 6.66 (m, 3H), 6.57 (s, 1H), 4.49 (t, J = 4.6 Hz, 1H), 3.87 (s, 3H), 3.85 (s, 3H), 3.83 (s, 3H), 3.38 (s, 3H), 2.98 – 2.75 (m, 2H), 2.15 – 2.04 (m, 2H); $^{13}$C NMR (150 MHz, $CDCl_3$) δ 150.73, 150.51, 146.44, 141.63, 137.82, 135.88, 130.60, 127.47, 124.30, 123.87, 119.66, 115.54, 110.25, 109.04, 72.68, 60.77, 60.32, 55.58, 55.38, 30.93, 19.85; HRMS (ES+) m/z found 372.1803 ($M+H^+$), while $C_{21}H_{26}NO_5$ ($M+H^+$) requires 372.1806.

**Quantum chemical calculation.** All of the quantum computations were performed using Gaussian 09.[26] First, the compounds were optimized at the ab initio B3LYP/6-31+G (d) and B3LYP/6-311++G (d,p) computational levels.[33] Frequency calculations were carried out to confirm that the obtained geometries corresponded to energetic minima. Then, TD-DFT at the same levels was used to calculate the vertical excitation energies. The frontier orbitals of the three molecules involved in the S0→S1 transitions were visualized using GaussView 5.0.

**Stability test.** The samples were dissolved in DMSO to a concentration of $1.5\times10^{-2}$ M. The sample solutions (4 mL) were irradiated using a high-power xenon lamp (Perfect Light PLS-SXE300, China) with a visible light filter under a nitrogen atmosphere. Next, HPLC (LC-20AD, Shimadzu, Japan, column ZORBAX Eclipse XDB-C18; mobile phase, methanol (70%)/$H_2O$; UV wavelength, absorbance at 254 nm) was used to measure changes in the sample and the percentages of the various components in the mixture. For the newly produced substances, LC-HRMS were used to determine the samples' structure.[29]

**Ultraviolet-visible spectrophotometric analysis.** For spectrophotometric analysis, suitable dilutions from working standard solutions of the compounds in DMSO ($1.0\times10^{-2}$ M) were generated ($1.4\times10^{-5}$ M). The prepared solutions were incubated in quartz cuvettes in a UV-vis spectrophotometer (SHIMADAZU UV-2600, Japan) and scanned over the range of 200-800 nm. The reference used for these measurements was DMSO.

**Assay for tumor cell growth inhibition.** Cytotoxic effects were examined in the SKOV3 human ovarian cancer and HT-29 human colon carcinoma cell lines by MTT assay. The absorbance at

570 nm was recorded on a fully automatic enzyme-labeled meter (Labsystems Inc. Wellscan MK-2, Finland). Compounds were tested in triplicate in at least three independent assays, and the average median inhibitory concentration (IC50) values were reported.[14, 34-36]

**Assay for Tubulin Polymerization Inhibition.** Bovine brain tubulin (Cytoskeleton, Inc., USA) (>99% pure, 3 mg/mL) in 100 μL of general tubulin buffer at 0 °C was placed in a half-area 96-well plate prewarmed at 37 °C in the presence of the tested compounds at varying concentrations. The reaction was started by warming the samples to 37 °C. The mass of polymer formed was monitored by turbidimetry at 340 nm every 1 min for 60 min with a multifunction microplate reader (Biotek Synergy 4, USA).[14, 34-36]

**Assay for *in vivo* antitumor activity.** BALB/c nude female mice (18−20 g) were obtained from Shanghai SLAC Laboratory Animal Co., Ltd. (Shanghai, China). Once the HT-29 xenografts reached a size of around 100 $mm^3$, mice were randomly assigned into appropriate groups (six animals/treatment and twelve animals for the control group). The drugs or vehicle were administered by ip injection once a day. After completing the treatment schedule and the evaluation period, tumor bearing mice were euthanized. Tumor volume (TV) was calculated by the formula: TV= $(ab^2)/2$ where $a$ is the length and $b$ is the width of the tumor nodules determined once per 3 days by caliper measurements and recorded along with body weights.[14]

## ASSOCIATED CONTENT

**Supporting Information**. The $^{1}$H NMR, $^{13}$C NMR, MS spectra, HPLC traces, and the X-ray crystal structure data of target compounds, crystallographic information files of compound **2**, and the molecular docking are available free of charge at http://pubs.acs.org.

## AUTHOR INFORMATION

**Corresponding Author**

*canhuizheng@smmu.edu.cn, cluo@mail.shcnc.ac.cn, juzhu@smmu.edu.cn and zhuoyoujun@smmu.edu.cn

**Author Contributions**

†These authors contributed equally.

**Funding Sources**

This work was supported by the National Natural Science Foundation of China (Grant No. 21172260, 30901859, 91229204 and 81230076), the "Chen Guang" project supported by the Shanghai Municipal Education Commission and the Shanghai Education Development Foundation (12CG42), and the Hi-Tech Research and Development Program of China (2012AA020302).

## ACKNOWLEDGMENTS

We thank Dr. Hao Guo of the Department of Chemistry, Fudan University, China for providing the light-stability testing and UV-vis spectrophotometric analysis equipment as well as helpful

discussions. We acknowledge the computation resources provided by the Computer Network Information Center, Chinese Academy of Sciences, and Shanghai Supercomputing Center.

## REFERENCES

1. Mikstacka, R.; Stefański, T.; Różański, J. Tubulin-interactive stilbene derivatives as anticancer agents. *Cell Mol Biol Lett* **2013,** 18, 368-397.

2. Spatafora, C.; Tringali, C. Natural-derived polyphenols as potential anticancer agents. *Anticancer Agents Med Chem* **2012,** 12, 902-918.

3. Jeandet, P.; Delaunois, B.; Conreux, A.; Donnez, D.; Nuzzo, V.; Cordelier, S.; Clément, C.; Courot, E. Biosynthesis, metabolism, molecular engineering, and biological functions of stilbene phytoalexins in plants. *BioFactors* **2010,** 36, 331-341.

4. Chong, J.; Poutaraud, A.; Hugueney, P. Metabolism and roles of stilbenes in plants. *Plant Sci* **2009,** 177, 143-155.

5. Roupe, K. A.; Remsberg, C. M.; Yáñez, J. A.; Davies, N. M. Pharmacometrics of stilbenes: seguing towards the clinic. *Curr Clin Pharmacol* **2006,** 1, 81-101.

6. Vang, O.; Ahmad, N.; Baile, C. A.; Baur, J. A.; Brown, K.; Csiszar, A.; Das, D. K.; Delmas, D.; Gottfried, C.; Lin, H.-Y. What is new for an old molecule? Systematic review and recommendations on the use of resveratrol. *PLoS One* **2011,** 6, e19881. doi: 10.1371/journal.pone.0019881.

7. Shan, Y. S.; Zhang, J.; Liu, Z.; Wang, M.; Dong, Y. Developments of combretastatin A-4 derivatives as anticancer agents. *Curr Med Chem* **2011,** 18, 523-538.

8. Tron, G. C.; Pirali, T.; Sorba, G.; Pagliai, F.; Busacca, S.; Genazzani, A. A. Medicinal chemistry of combretastatin A4: present and future directions. *J Med Chem* **2006,** 49, 3033-3044.

9. Siemann, D. W.; Chaplin, D. J.; Walicke, P. A. A review and update of the current status of the vasculature-disabling agent combretastatin-A4 phosphate (CA4P). *Expert Opin Investig Drugs* **2009,** 18, 189-197.

10. Nguyen, T. L.; McGrath, C.; Hermone, A. R.; Burnett, J. C.; Zaharevitz, D. W.; Day, B. W.; Wipf, P.; Hamel, E.; Gussio, R. A common pharmacophore for a diverse set of colchicine site inhibitors using a structure-based approach. *J Med Chem* **2005,** 48, 6107-6116.

11. Rajak, H.; Kumar Dewangan, P.; Patel, V.; Kumar Jain, D.; Singh, A.; Veerasamy, R.; Chander Sharma, P.; Dixit, A. Design of Combretastatin A-4 Analogs as Tubulin Targeted Vascular Disrupting Agent with Special Emphasis on Their Cis-Restricted Isomers. *Curr Pharm Des* **2013,** 19, 1923-1955.

12. Cushman, M.; Nagarathnam, D.; Gopal, D.; Chakraborti, A. K.; Lin, C. M.; Hamel, E. Synthesis and evaluation of stilbene and dihydrostilbene derivatives as potential anticancer agents that inhibit tubulin polymerization. *J Med Chem* **1991,** 34, 2579-2588.

13. Cushman, M.; Nagarathnam, D.; Gopal, D.; He, H. M.; Lin, C. M.; Hamel, E. Synthesis and evaluation of analogs of (Z)-1-(4-methoxyphenyl)-2-(3, 4, 5-trimethoxyphenyl) ethene as potential cytotoxic and antimitotic agents. *J Med Chem* **1992,** 35, 2293-2306.

14. Liu, J.; Zheng, C. H.; Ren, X. H.; Zhou, F.; Li, W.; Zhu, J.; Lv, J. G.; Zhou, Y. J. Synthesis and biological evaluation of 1-benzylidene-3,4-dihydronaphthalen-2-one as a new class of microtubule-targeting agents. *J Med Chem* **2012,** 55, 5720-5733.

15. Jorgensen, W. L. The many roles of computation in drug discovery. *Science* **2004,** 303, 1813-1818.

16. Zhou, T.; Huang, D. Z.; Caflisch, A. Quantum Mechanical Methods for Drug Design. *Curr Top Med Chem* **2010,** 10, 33-45.

17. Kim, J. T.; Hamilton, A. D.; Bailey, C. M.; Domoal, R. A.; Wang, L. G.; Anderson, K. S.; Jorgensen, W. L. FEP-guided selection of bicyclic heterocycles in lead optimization for non-nucleoside inhibitors of HIV-1 reverse transcriptase. *J Am Chem Soc* **2006,** 128, 15372-15373.

18. Plötner, J.; Dreuw, A. Molecular Mechanism of the Z/E-Photoisomerization of Hemithioindigo Hemistilbene†. *J Phys Chem A* **2009,** 113, 11882-11887.

19. Lewis, F. D.; Weigel, W. Excited State Properties of Donor-Acceptor Substituted trans-Stilbenes: The m eta-Amino Effect. *J Phys Chem A* **2000,** 104, 8146-8153.

20. Bearpark, M. J.; Bernardi, F.; Clifford, S.; Olivucci, M.; Robb, M. A.; Vreven, T. Cooperating rings in cis-stilbene lead to an S0/S1 conical intersection. *J Phys Chem A* **1997,** 101, 3841-3847.

21. Cao, C.; Chen, G.; Wu, Y. Effects of substituent and solvent on the UV absorption energy of 4, 4′ -disubstituted stilbenes. *Sci China Chem* **2011,** 54, 1735-1744.

22. Oshkin, I.; Budyka, M. Quantum-chemical study of the photoisomerization and photocyclization reactions of styrylquinolines: Potential energy surfaces. *High Energ Chem* **2010,** 44, 472-481.

23. Fleming, G. R.; Courtney, S. H.; Balk, M. W. Activated barrier crossing: Comparison of experiment and theory. *J Stat Phys* **1986,** 42, 83-104.

24. Schultz, T.; Quenneville, J.; Levine, B.; Toniolo, A.; Martínez, T. J.; Lochbrunner, S.; Schmitt, M.; Shaffer, J. P.; Zgierski, M. Z.; Stolow, A. Mechanism and dynamics of azobenzene photoisomerization. *J Am Chem Soc* **2003,** 125, 8098-8099.

25. Quenneville, J.; Martínez, T. J. Ab initio study of cis-trans photoisomerization in stilbene and ethylene. *J Phys Chem A* **2003,** 107, 829-837.

26. Gaussian09. *Gaussian, Inc.: Wallingford, CT.*

27. Zhou, Y. J.; Liu, J.; Zheng, C. H.; Zhou, F.; Ren, X. H.; Zhu, J.; Lv, J. G.; Liu, N. 1-substituted benzylidene-2-naphthalenone derivative, preparation method thereof and use thereof. *C.N. Pat. Appl. 20121495034* **2012**.

28. Zhu, J.; Zhou, Y. J.; Zheng, C. H.; Jiang, J. H.; Lv, J. G.; Liu, J.; Zhou, H. Substituted benzylidene-naphthalenone derivative, preparation method thereof and use thereof *C.N. Pat. Appl. 201510064131* **2015**.

29. Pandit, B.; Sun, Y.; Chen, P.; Sackett, D. L.; Hu, Z.; Rich, W.; Li, C.; Lewis, A.; Schaefer, K.; Li, P.-K. Structure–activity-relationship studies of conformationally restricted analogs of combretastatin A-4 derived from SU5416. *Bioorg Med Chem* **2006,** 14, 6492-6501.

30. Skoog, D. A.; Holler, F. J.; Crouch, S. R. *Principles of Instrumental Analysis Sixth Edition* Thomson Corporation: CA, 2007.

31. Lawrence, N. J.; Hepworth, L. A.; Rennison, D.; McGown, A. T.; Hadfield, J. A. Synthesis and anticancer activity of fluorinated analogues of combretastatin A-4. *Journal of fluorine chemistry* **2003,** 123, 101-108.

32. Gaukroger, K.; Hadfield, J. A.; Lawrence, N. J.; Nolan, S.; McGown, A. T. Structural requirements for the interaction of combretastatins with tubulin: how important is the trimethoxy unit? *Organic & biomolecular chemistry* **2003,** 1, 3033-3037.

33. Frisch, M. J.; Pople, J. A.; Binkley, J. S. Self‐consistent molecular orbital methods 25. Supplementary functions for Gaussian basis sets. *The Journal of chemical physics* **1984,** 80, 3265-3269.

34. Morris, G. M.; Huey, R.; Lindstrom, W.; Sanner, M. F.; Belew, R. K.; Goodsell, D. S.; Olson, A. J. AutoDock4 and AutoDockTools4: Automated docking with selective receptor flexibility. *J Comput Chem* **2009,** 30, 2785-2791.

35. Li, Y. W.; Liu, J.; Liu, N.; Shi, D.; Zhou, X. T.; Lv, J. G.; Zhu, J.; Zheng, C. H.; Zhou, Y. J. Imidazolone-amide bridges and their effects on tubulin polymerization in cis-locked vinylogous combretastatin-A4 analogues: synthesis and biological evaluation. *Bioorg Med Chem* **2011,** 19, 3579-3584.

36. Zheng, C. H.; Chen, J.; Liu, J.; Zhou, X. T.; Liu, N.; Shi, D.; Huang, J. J.; Lv, J. G.; Zhu, J.; Zhou, Y. J. Synthesis and biological evaluation of 1-phenyl-1,2,3,4-dihydroisoquinoline compounds as tubulin polymerization inhibitors. *Arch Pharm (Weinheim)* **2012,** 345, 454-462.

**Graphic for manistript**